Makara Journal of Science

Volume 25
Issue 3 *September*

Article 1

9-30-2021

Hemoglobin-Modified Core–Shell Fe3O4@Au Nanostructures for the Electrochemical Detection of Acrylamide

Endang Saepudin
Department of Chemistry, Faculty of Mathematics and Natural Sciences, Universitas Indonesia, Depok 16424, Indonesia

Tri Yuliani
Department of Chemistry, Faculty of Mathematics and Natural Sciences, Universitas Indonesia, Depok 16424, Indonesia

Mochammad Arfin Fardiansyah Nasution
Department of Chemistry, Faculty of Mathematics and Natural Sciences, Universitas Indonesia, Depok 16424, Indonesia

Munawar Khalil
Department of Chemistry, Faculty of Mathematics and Natural Sciences, Universitas Indonesia, Depok 16424, Indonesia

Jong Wook Hong
Department of Chemistry, University of Ulsan, Ulsan 44776, South Korea

Follow this and additional works at: https://scholarhub.ui.ac.id/science

 Part of the Analytical Chemistry Commons, Materials Chemistry Commons, and the Other Chemistry Commons

See next page for additional authors

Recommended Citation

Saepudin, Endang; Yuliani, Tri; Nasution, Mochammad Arfin Fardiansyah; Khalil, Munawar; Hong, Jong Wook; and Ivandini, Tribidasari Anggraningrum (2021) "Hemoglobin-Modified Core–Shell Fe3O4@Au Nanostructures for the Electrochemical Detection of Acrylamide," *Makara Journal of Science*: Vol. 25 : Iss. 3 , Article 1.
DOI: 10.7454/mss.v25i3.1232
Available at: https://scholarhub.ui.ac.id/science/vol25/iss3/1

This Article is brought to you for free and open access by the Universitas Indonesia at UI Scholars Hub. It has been accepted for inclusion in Makara Journal of Science by an authorized editor of UI Scholars Hub.

Hemoglobin-Modified Core–Shell Fe3O4@Au Nanostructures for the Electrochemical Detection of Acrylamide

Authors

Endang Saepudin, Tri Yuliani, Mochammad Arfin Fardiansyah Nasution, Munawar Khalil, Jong Wook Hong, and Tribidasari Anggraningrum Ivandini

This article is available in Makara Journal of Science: https://scholarhub.ui.ac.id/science/vol25/iss3/1

Makara Journal of Science, 25/3 (2021), 127–134
doi: 10.7454/mss.v25i3.1232

Hemoglobin-Modified Core–Shell Fe_3O_4@Au Nanostructures for the Electrochemical Detection of Acrylamide

Endang Saepudin[1], Tri Yuliani[1], Mochammad Arfin Fardiansyah Nasution[1], Munawar Khalil[1], Jong Wook Hong[2], and Tribidasari Anggraningrum Ivandini[1*]

1. Department of Chemistry, Faculty of Mathematics and Natural Sciences, Universitas Indonesia, Depok 16424, Indonesia
2. Department of Chemistry, University of Ulsan, Ulsan 44776, South Korea

[*]*E-mail: ivandini.tri@sci.ui.ac.id*

Received April 10, 2021 | Accepted August 20, 2021

Abstract

In this study, electrochemical detection of acrylamide using hemoglobin (Hb)-modified core–shell Fe_3O_4@Au nanostructures was conducted. Fe_3O_4 nanoparticles (~4.9 nm) and core–shell Fe_3O_4@Au (5.0–6.4 nm) nanostructures were successfully synthesized by the thermal decomposition method. Electrochemical investigation revealed that the optimum amount of Hb of 2 mg/mL could be immobilized in 0.1 M acetate buffer solution (pH = 6). Moreover, the detection of acrylamide using Fe_3O_4@Au/Hb was evaluated by the cyclic voltammetry technique. A linear calibration curve (R^2 = 0.98) in the concentration range of 0.1 to 1.0 µM could be achieved with an estimated limit of detection, limit of quantification, and sensitivity of 0.136 µM, 0.453 µM, and 0.4411 µA/µM, respectively. Furthermore, the developed biosensor exhibited high selectivity in the presence of ascorbic acid, melamine, and caffeine. The developed biosensor was applied to the detection of acrylamide in coffee samples and validated using the standard high-performance liquid chromatography (HPLC) method. The concentration of acrylamide in coffee samples was determined to be 37.450 and 35.377 ppm using electrochemical measurement and HPLC, respectively.

Keywords: acrylamide, core–shell, electrochemical detection, Fe_3O_4@Au, hemoglobin

Introduction

Acrylamide, a carcinogen and neurotoxin, is primarily present in various sugar-containing and carbohydrate-containing foods processed at high temperatures [1, 2]. However, the current analytical tools used to detect acrylamide in food samples, such as liquid chromatography–tandem mass spectrometry [3], high-performance liquid chromatography (HPLC) [4], headspace solid-phase microextraction, and gas chromatography–flame ionization detection [5], have several drawbacks, including high cost and sample preparation complexity. Therefore, the development of methods for detecting acrylamide that are easy, inexpensive, and fast is important to monitor healthy foods in the community. One of the methods employed to overcome the previously mentioned problems is the development of a biosensor, which is often combined with electrochemical techniques because of its high selectivity and sensitivity [6]. Recently, hemoglobin (Hb)-based biosensors have attracted considerable interest in the development of methods for detecting acrylamide [7–9].

Hb is a redox-active protein involving four polypeptide chains, and each polypeptide chain has one Fe^{3+} electroactive heme group. Hb electroactivity is associated with the reversible conversion of Hb-Fe^{3+} into Hb-Fe^{2+}. The Hb functional groups are not easily oxidized or reduced in plain bare electrodes because of the slow transfer of electrons caused by the large three-dimensional structure of Hb [8]. This large structure leads to the possibility of the Hb orientation being inappropriate for the surface of the electrode and increases the distance between the center of the heme and the surface of the electrode [10]. Moreover, the polarity difference between the nonpolar groups on the surface of the carbon electrode and polar groups in one of the Hb functional groups results in weak adsorption [11]. To produce biosensors with proteins (such as Hb), the electrochemical contact between active redox proteins (Hb) and transducers (electrodes) needs to be maintained. Biosensors can respond directly to oxidation in Hb; however, electron transfer occurs slowly, resulting in a weak signal response [12]. The problem of slow electron transfer caused by protein adsorption and electrode passivity is overcome using various electro-

mediators, including Ag, Au, Pt, Pd, Ir, Rh, Ag/Au, Pt/Ag, and Pt/Ag [9].

In this study, electrochemical biosensors were developed by combining screen printing technology and nanotechnology. Nanoparticles can play an important role in improving sensor performance because of their large specific surface area, excellent conductivity, and compatibility. The use of nanoparticles for electrochemical sensors has been widely reported [13–16]. Among all types of nanoparticles, superparamagnetic iron oxide nanoparticles, particularly Fe_3O_4NP, have attracted considerable attention because of their unique magnetic properties and their capability to be easily chemically modified to increase biocompatibility and dispersibility [17]. Meanwhile, the synthesis of noble metal nanostructures is interesting because of their chemical, physical, and catalytic properties [18]. In this context, bimetallic nanostructures exhibit significantly improved optical, catalytic, and electrical properties of each monometallic constituent [19]. A previous study reported that Au-Fe_3O_4NP was more active than the single-component AuNP or Fe_3O_4NP [20]. The increased activity can be attributed to the partial charge transfer between Au and Fe_3O_4 at the nanoscale particle interface [20].

In this study, Hb-modified core–shell Fe_3O_4@Au nanoparticles were prepared for the electrochemical detection of acrylamide. The observed decrease in the current responses due to the formation of Hb–acrylamide (Hb-AA) adduct was used as the signals. A linear calibration curve in various concentrations of acrylamide could be achieved, indicating that the developed method was promising for the detection of acrylamide.

Material and Methods

Materials and instruments. Iron(III) hexahydrate ($FeCl_3 \cdot 6H_2O$, 98%; Sigma-Aldrich, St. Louis, MO, USA), sodium oleate ($C_{13}H_{33}NaO_2$, 97%; Tokyo Chemical Industry Co., Ltd., Tokyo, Japan), oleic acid ($C_8H_{32}O_2$, 90%; Sigma-Aldrich, St. Louis, MO, USA), gold(III) chloride trihydrate ($HAuCl_4 \cdot 3H_2O$, 99%; Sigma-Aldrich, St. Louis, MO, USA), oleylamine ($C_{18}H_{37}N$, 70%; Sigma-Aldrich, St. Louis, MO, USA), acrylamide (C_3H_5NO, 99%; Sigma-Aldrich, St. Louis, MO, USA), glucose ($C_6H_{12}O_6$, 99%; Wako Pure Chemical Inc., Osaka, Japan), sodium acetate ($C_2H_3NaO_2$, 99%; Merck Inc., Darmstadt, Germany), caffeine ($C_8H_{10}N_4O_2$, 99%; Wako Pure Chemical Inc., Osaka, Japan), melamine ($C_3H_6N_6$, 99%; Wako Pure Chemical Inc., Osaka, Japan), and ascorbic acid ($C_6H_8O_6$, 99%; Wako Pure Chemical Inc., Osaka, Japan) were purchased in reagent grade. Meanwhile, distilled water was obtained with a resistivity >18.2 MΩ·cm. Transmission electron microscopy (TEM) images were obtained using a Jeol JEM-2100F (University of Ulsan, Ulsan, South Korea). Inductively coupled plasma–optical emission spectrometry (ICP-OES) measurement was conducted using a SPECTROBLUE ICP-OES (Ametek; University of Ulsan, Ulsan, South Korea). X-ray diffraction (XRD) measurement was conducted using a Rigaku D/Max 2500V/PC scanning in the 2θ range of 30° to 90° (University of Ulsan, Ulsan, South Korea). Scanning electron microscopy (SEM) images were obtained using a Zeiss EVO M10 (DropSens μStat 400 S/N: UST0157400; Universitas Indonesia, Depok, West Java, Indonesia).

Synthesis of Fe_3O_4@AuNP and Fe_3O_4@Au/Hb. Fe_3O_4NP was synthesized by the thermal decomposition method according to the method proposed by Kim *et al*. with some modifications [21]. Fe_3O_4NP was prepared using the iron oleate complex as the precursor. This complex was synthesized by dissolving $FeCl_3 \cdot 6H_2O$ (5.4 g) and sodium oleate (18.25 g) in 26.67 mL ethanol, 30 mL distilled water, and 70 mL hexane. This mixture was heated at 70 ℃ for 4 h. After the reaction was completed, the reddish brown top layer containing the organic compound was separated and washed with distilled water several times to remove NaCl and unreacted monomers. The iron oleate complex (18 g) and oleic acid (3.56 mL) were dissolved in 1-octadecene (100 g) through vigorous stirring. Then, the reaction temperature was increased to 320 °C at a heating rate of 3.3 °C/min and maintained at this temperature for 30 min under atmospheric nitrogen. During the reaction, the brownish red color turned to dark brown. After cooling the mixture to room temperature, the products were washed with ethanol and hexane and dried.

Fe_3O_4@AuNP was prepared according to the procedure proposed by Sun *et al*. with some modifications [16] by dropwise mixing of 10 mL chloroform containing 40 mg Fe_3O_4NP and 2 mmol oleylamine with various concentrations of gold solutions. All variations were stirred for 20 h. Ethanol was added to the precipitation. Then, the precipitation was washed with hexane and ethanol several times and dried under vacuum. The product was dissolved in an aqueous solution containing 0.1 M cetyltrimethylammonium bromide and 0.1 mM sodium citrate. After 10 min sonication, Fe_3O_4@AuNP formed a pink solution. Characterization was performed using TEM, XRD, and inductively coupled plasma–mass spectrometry (ICP-MS). To prepare Fe_3O_4@Au/Hb, 1 mg Fe_3O_4@AuNP was incubated in Hb solutions at 37 °C for 4 h. Various buffers (i.e., acetate buffer solution and phosphate buffer solution (PBS)), pH values (i.e., 4, 5, 6, 7, and 8), and Hb concentrations (i.e., 2, 4, 6, 8, and 10 mg/mL) were investigated to achieve high electrochemical signal currents.

Electrochemical detection of acrylamide. Various concentrations of standard acrylamide solutions (0.01-0.1 μM) were added to 1 mL Fe_3O_4@AuNP/Hb. After sonication, the precipitate (Fe_3O_4@AuNP/Hb-AA) was separated using external magnets and redispersed in 10

mL of 0.1 M PBS pH 6. A 40 µL volume of these solutions was measured using the cyclic voltammetry (CV) technique on a screen-printed carbon electrode (SPCE) in the potential range −0.8 V to +0.8 V at a scan rate of 50 mV/s. These steps were repeated three times. The selectivity of the developed biosensor was evaluated against other compounds that are commonly found in coffee samples, including caffeine, melamine, and ascorbic acid, at the concentration of 0.1 µM in 0.1 µM acrylamide solutions.

Coffee sample measurements. The Lampung coffee powder sample was treated according to the technique proposed in Ref. [22] with some modifications. First, 1.1 g coffee powder and 10 mL *n*-hexane were added to the sample and mixed in a vortex for 5 min. The residue was separated and dried in an oven at 60 °C for 1 h. Then, the residue was sonicated in a mixture of 10 mL acetone and 50 µL distilled water for 20 min. The acetone layer was filtered using filter paper and evaporated in a water bath. Next, the residue was dissolved in 10 mL of a mixture solution of acetonitrile and distilled water (5:95, v/v), shaken, and filtered with a 0.45 µm filter disk. The acrylamide content in coffee samples was measured using the CV technique under the optimum conditions. Validation of the method was performed using the HPLC technique [23]. A 20 µL volume of various concentrations of acrylamide standard solutions (10–250 ppm) and coffee samples were measured using the HPLC system. The mobile phase used was a mixture solution of acetonitrile and distilled water (5:95, v/v). The flow rate was 1 mL/min at the wavelength of 284 nm.

Results and Discussion

Synthesis of Fe_3O_4@AuNP. The XRD pattern of the as-synthesized Fe_3O_4 NP (Figure 1) shows peak broadening, which is generally observed when the particle size is small. The diffractogram shows poor crystallinity, and peaks are hardly visible above the noise because of the nanoparticles of various oxygen contents (multiple phases) [24]. However, the signals can be assigned to a spectrum of spinel. The TEM image (inset of Figure 1) shows that particles of ~5 nm could be formed.

Then, the prepared Fe_3O_4 nanoparticles were used as the precursors to synthesize Fe_3O_4@AuNP by mixing with $HAuCl_4 \cdot 3H_2O$ solution. Fe_3O_4 could act as the core, whereas the gold solutions could act as the shell precursors. The same concentrations of the core were used with various concentrations of the shell, as shown in Table 1. The color changes the mixture from brownish black to pink indicated the formation of a gold shell. The TEM images (Figure 2a-2d) indicate that all variations of gold (shell) and Fe_3O_4 (core) ratios formed monodisperse particles with narrow particle size distributions (standard deviation of less than 10%). Further characterization using XRD spectrum (Figure 2e) indicated that the centered cubic phase of Fe_3O_4NP was coated with a layer of crystalline gold.

To prepare the water-soluble nanoparticles, the dried Fe_3O_4@AuNP was dissolved in an aqueous solution containing 0.1 M cationic surfactant combination (CTAB) and 0.1 mM sodium citrate. Sodium citrate can attach to Au and stabilize nanoparticles by giving a negative charge to the surface of Fe_3O_4@AuNP. Sun *et al*. reported that sodium citrate alone cannot stabilize Fe_3O_4@AuNP in water, whereas the CTAB with citrate can stabilize Fe_3O_4@AuNP by forming a double layer on the surface of nanoparticles [25]. This CTAB/citrate method can dissolve AuNP encapsulated by oleylamine, but cannot be used for Fe_3O_4NP. The dissolution of the nanoparticles indicated that the nanoparticles have been encapsulated by Au or Fe_3O_4@AuNP is successfully formed. Furthermore, confirmation using the ICP-MS data (Table 1) showed that the use of various concentrations of gold solutions as the precursors produced different mole ratios of Fe_3O_4 as the core and gold as the shell.

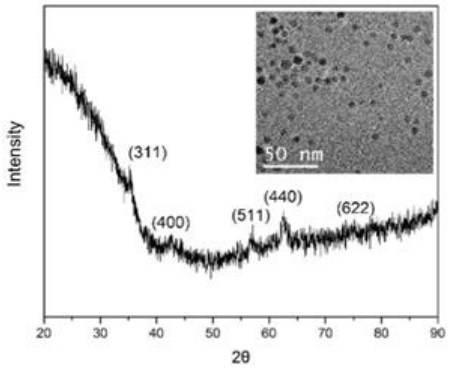

Figure 1. X-ray Diffraction Pattern of Fe_3O_4NP with the Transmission Electron Microscopy Images of the Nanoparticles in the Inset

Table 1. Summary of the Mole Ratios of Fe_3O_4/Au Synthesized using Various Concentrations of Gold Solutions as the Precursors

Variation	10 mM $HAuCl_4 \cdot 3H_2O$ (mL)	Distilled Water (mL)	Oleylamine (µL)	Mole Ratios of Fe_3O_4/Au	Average Particle Size (nm)
a	2.5	7.5	4.71	30:1	5.0
b	5	5	9.43	3:2	5.6
c	7.5	2.5	14.15	3:4	5.7
d	10	–	18.87	1:3	6.4

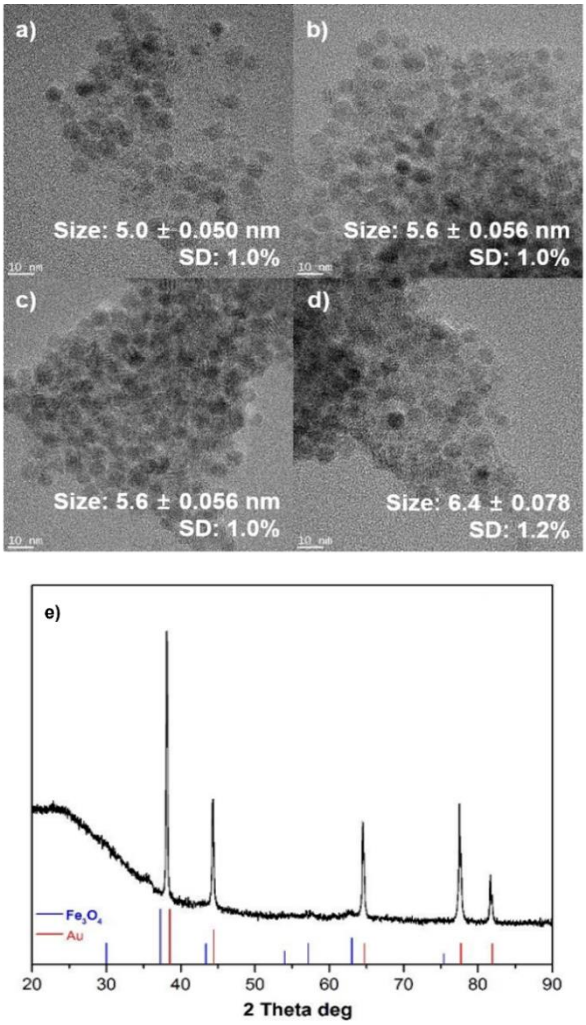

Figure 2. TEM Images of (a–d) Fe_3O_4@AuNP with Various Ratios of Fe_3O_4/Au and (e) its Representative XRD Patterns

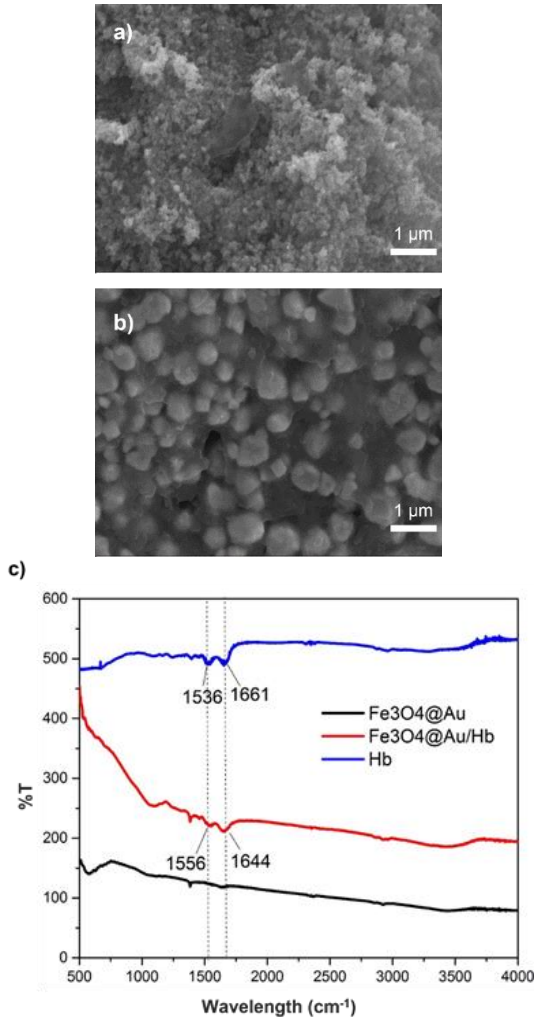

Figure 3. SEM Images of (a) Fe_3O_4@AuNP and (b) Fe_3O_4@AuNP/Hb and (c) the Related Infrared Spectra of Fe_3O_4@AuNP, Fe_3O_4@AuNP/Hb, and Hb

Modification of Fe_3O_4@AuNP with Hb. The SEM images of Fe_3O_4@AuNP before and after modification with Hb (Figure 3a and Figure 3b, respectively) show that the particle size significantly increases after modification. Notably, Hb has self-assembled on the surface of Fe_3O_4@AuNP to form the globular morphology of Fe_3O_4@AuNP. Confirmation using Fourier transform infrared spectroscopy after modification (Figure 3c) showed a vibration peak of amide I (1,600–1,700 cm^{-1}) attributed to C=O vibration of the peptide bond and a vibration peak of amide II (1,500–1,620 cm^{-1}) attributed to the combination of NH stretching vibrations and C–N group vibration peptides [26]. Slight shifts observed at the wavelength of both vibration peaks in amide I and amide II were attributed to the bond between Au and $–NH_2$ groups.

Electrochemical studies of Fe_3O_4@AuNP/Hb. The CV technique on SPCE was applied to analyze the electrochemical behavior of Fe_3O_4@AuNP/Hb. The voltammograms shown in Figure 4a indicate that an oxidation peak at ~0.1 V related to the oxidation of Fe^{2+} to Fe^{3+} was observed in all types of Fe_3O_4@AuNP/Hb (Table 1), except for nanoparticles with a Fe_3O_4/Au mole ratio of 1:3. When gold fully covered the Fe_3O_4NP surface, this peak disappeared. Optimization of the amount of Hb immobilized in Fe_3O_4@AuNP was performed with a Fe_3O_4/Au mole ratio of 1:3. Various concentrations of Hb were added to the nanoparticles. The cyclic voltammograms shown in Figure 4b indicate that the highest current peak at approximately 0.1 V was observed at the Hb concentration of 2 mg/mL. Therefore, the Fe_3O_4/Au mole ratio of 1:3 and Hb concentration of 2 mg/mL were used for the subsequent experiments.

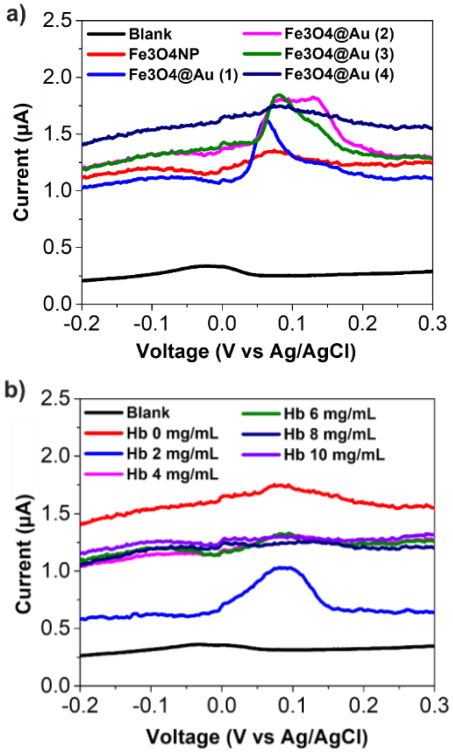

Figure 4. Voltammograms of Fe_3O_4@AuNP/Hb in 0.1 M PBS pH 6 (a) with Various Ratios of Fe_3O_4/Au and (b) in Various Concentrations of Hb. The Scan Rate was 50 mV/s

Electrochemical responses of acrylamide using Fe_3O_4@AuNP/Hb on SPCE. The reaction of Hb with acrylamide causes the formation of Hb-AA adduct, which can change the electroactivity of Hb. Accordingly, signal responses were collected according to the decrease in the Fe_3O_4@AuNP/Hb currents. Figure 5 shows the voltammograms of Fe_3O_4@AuNP/Hb obtained in various concentrations of acrylamide in 0.1 M PBS pH 6. A linear calibration curve (y = −0.4411 (μM) + 0.8206, r = 0.9805, n = 7) in the range of 0 to 1 μM of AA was obtained using CV with an estimated limit of detection (LOD, S/N = 3) and limit of quantification (LOQ, S/N = 10) of 0.136 and 0.453 μM, respectively. Good repeatability was observed with an RSD (n = 5) value of 4.17%.

The selectivity of the method was examined in the presence of ascorbic acid, melamine, and caffeine in acrylamide samples. The cyclic voltammograms of 0.1 μM acrylamide solutions in the presence of 0.1 μM of each impurity did not show a new oxidation or reduction peak. However, a 5.4% increase in the oxidation current was observed in the presence of caffeine. Meanwhile, increasing currents of 17.4% and 31.4% were observed in the presence of ascorbic acid and melamine, respectively. These results indicated the decrease in the acrylamide–Hb interaction in the systems because of the impurities.

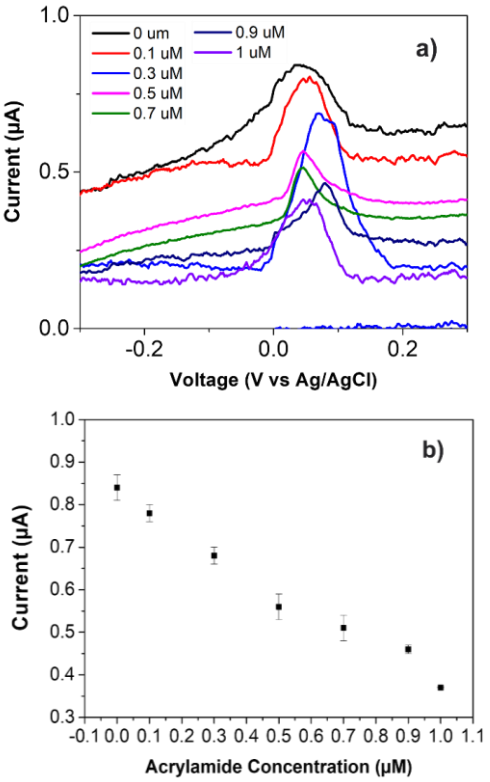

Figure 5. (a) Voltammograms of Fe_3O_4@AuNP/Hb in Various Concentrations of Acrylamide in 0.1 M PBS pH 6 and (b) its Related Calibration Curve. The Scan Rate was 50 mV/s

Acrylamide measurements in coffee powder samples. Solutions of commercial coffee powder samples were prepared and analyzed using the developed method. A typical voltammogram of sample measurement is shown in Figure 6a. The average current of three measurements of 0.802 μA was obtained from the voltammograms. The conversion of 50 dilutions resulted in the acrylamide content in coffee samples of 37.450 ppm. According to the Food and Drug Administration, the tolerable amount of acrylamide intake is 2.6 μg/kg BW/day to avoid carcinogenic risk. If the average body weight of adult women and men is assumed to be approximately 40–80 kg, then the tolerable amount of acrylamide intake is 104–208 μg/day.

HPLC was utilized to validate the method. The chromatograms of various concentrations of acrylamide in the concentration range 10-2,500 ppm shown in Figure 7a indicate that the standard acrylamide has a retention time of 3.1 min. The intensity was linear to the concentrations (R^2 = 0.998) with the equation of y = 46.587x + 1,609.6. Meanwhile, the chromatograms of the coffee samples showed several peaks at different retention times, indicating that some other compounds were present in the coffee samples. The chromatograms showed that acrylamide is not the main constituent of coffee as the peak at the retention time of 3.1 min has a

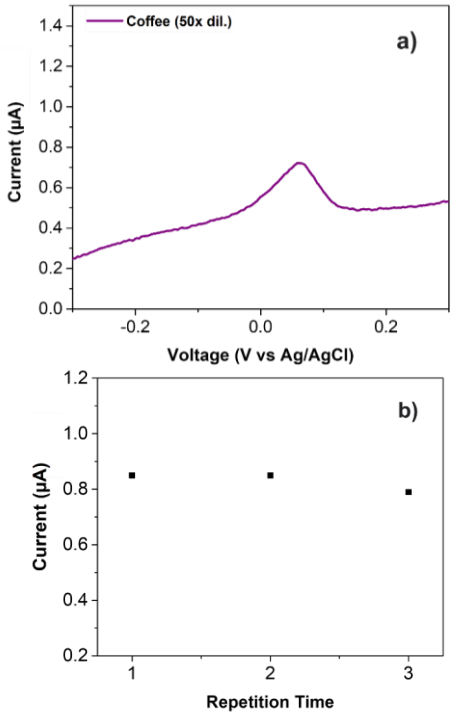

Figure 6. (a) Voltammograms and (b) Current Plots of Coffee Samples Measured using the Developed Fe_3O_4@AuNP/Hb on a Screen-Printed Carbon Electrode

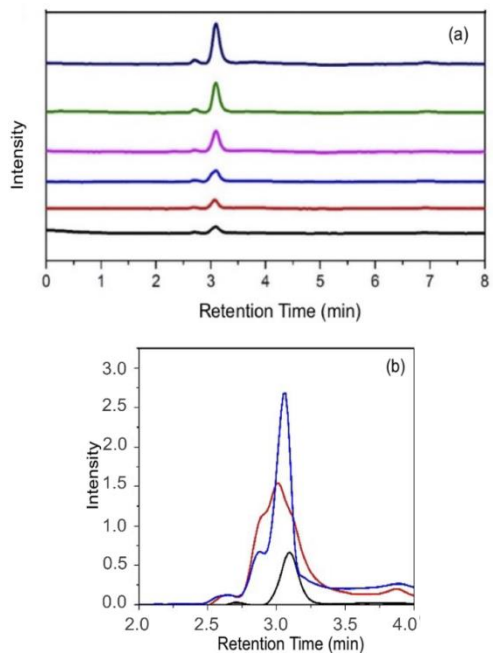

Figure 7. (a) Chromatograms of Various Concentrations of Acrylamide Standard Solutions and (b) Chromatograms of Coffee Samples without (Black Line) and with (Blue Line) the Addition of 100 ppm Acrylamide Standard in Comparison with the Chromatograms of 100 ppm Acrylamide Standard (Black Line)

significantly lower visible intensity than the other peaks (Figure 7b, red line). The comparison of this chromatogram with that of 100 ppm acrylamide standard solution (black line) and that with the addition of 100 ppm standard acrylamide in the coffee samples (blue line) confirmed that acrylamide was present in the coffee samples. Based on the calculated results, the sample concentration was determined to be 35.377 ppm.

Conclusion

Fe_3O_4 nanoparticles were successfully synthesized by the thermal decomposition method using the iron oleate complex as the precursor with a particle size of ~4.9 nm. Modification with CTAB and citrate increased the hydrophilicity of Fe_3O_4NP. Accordingly, Fe_3O_4NP has been successfully coated with various concentrations of gold solutions. Increasing the concentration of the gold solution, which is used as the precursor, increased the thickness of the gold shell. The optimum Fe_3O_4/Au ratio of 1:3 with 2 mg/mL Hb in 0.1 M PBS pH 6 yielded acrylamide responses with good linearity at a concentration range of 0 to 1.0 µM. The LOD, LOQ, and sensitivity of 0.136 µM, 0.453 µM, and 0.4411 µA/µM, respectively, could be achieved. Finally, the detection of acrylamide in coffee samples exhibited high sensitivity and applicability, indicating that the developed sensor is promising.

Acknowledgements

The Authors acknowledge the support from the Directorate of Research and Community Engagements, Universitas Indonesia through the Penelitian Tesis Magister 2020 (Grant No. NKB-495/UN2.RST/HKP.05.00/2020) funded by the Ministry of Research and Technology/National Research and Innovation Agency, Republic of Indonesia. There are no conflicts of interest to declare.

References

[1] Asnaashari, M., Kenari, R.E., Farahmandfar, R., Abnous, K., Taghdisi, S.M. 2019. An electrochemical biosensor based on hemoglobin-oligonucleotides-modified electrode for detection of acrylamide in potato fries. Food Chem. 271(2018): 54–61, http://dx.doi.org/10.1016/j.foodchem.2018.07.150.

[2] González-Fuentes, F.J., Manríquez, J., Godínez, L.A., Escarpa, A., Mendoza, S. 2014. Electrochemical analysis of acrylamide using screen-printed carboxylated single-walled carbon nanotube electrodes. Electroanal. 26(5): 1039–1044, http://dx.doi.org/10.1002/elan.201300636.

[3] Jozinović, A., Šarkanj, B., Ačkar, D., Balentić, J.P., Šubarić, D., Cvetković, T., Ranilović, J., Guberac, S., Babić, J. 2019. Simultaneous determination of acrylamide and hydroxymethylfurfural in extruded

products by LC-MS/MS method. Mol. 24(10): 1–13, http://dx.doi.org/10.3390/molecules24101971.

[4] Champrasert, O., Chu, J., Meng, Q., Viney, S., Holmes, M., Suwannaporn, P., Orfila, C. 2021. Inhibitory effect of polysaccharides on acrylamide formation in chemical and food model systems. Food Chem. 363(May): 130213, http://dx.doi.org/10.1016/j.foodchem.2021.130213.

[5] Ghiasvand, A.R., Hajipour, S. 2016. Direct determination of acrylamide in potato chips by using headspace solid-phase microextraction coupled with gas chromatography-flame ionization detection. Talanta. 146: 417–422, http://dx.doi.org/10.101 6/j.talanta.2015.09.004.

[6] Mishra, G.K., Barfidokht, A., Tehrani, F., Mishra, R.K. 2018. Food safety analysis using electrochemical biosensors. Foods. 7(9): 141, http://dx.doi.org/10.3390/foods7090141.

[7] Li, N., Liu, X., Zhu, J., Zhou, B., Jing, J., Wang, A., Xu, R., Wen, Z., Shi, X., Guo, S. 2020. Simple and sensitive detection of acrylamide based on hemoglobin immobilization in carbon ionic liquid paste electrode. Food Cont. 109(2019): 1–6, http://dx.doi.org/10.1016/j.foodcont.2019.106764.

[8] Wulandari, R., Ivandini, T.A., Irkham, Saepudin, E., Einaga, Y. 2019. Modification of boron-doped diamond electrodes with platinum to increase the stability and sensitivity of haemoglobin-based acrylamide sensors. Sensors Mater. 31(4): 1105–1117, http://dx.doi.org/10.18494/sam.2019.2192.

[9] Garabagiu, S., Mihailescu, G. 2011. Simple hemoglobin-gold nanoparticles modified electrode for the amperometric detection of acrylamide. J. Electroanal. Chem. 659(2): 196–200, http://dx.doi.org/10.1016/j.jelechem.2011.06.003.

[10] Yáñez-Sedeño, P., Pingarrón, J.M. 2005. Gold nanoparticle-based electrochemical biosensors. Anal. Bioanal. Chem. 382(4): 884–886, http://dx.doi.org/10.1007/s00216-005-3221-5.

[11] Ren, L., Dong, J., Cheng, X., Xu, J., Hu, P. 2013. Hydrogen peroxide biosensor based on direct electrochemistry of hemoglobin immobilized on gold nanoparticles in a hierarchically porous zeolite. Microchim. Acta. 180(13–14): 1333–1340, http://dx.doi.org/10.1007/s00604-013-1064-x.

[12] Nekrassova, O., Lawrence, N.S., Compton, R.G. 2004. Selective electroanalytical assay for cysteine at a boron doped diamond electrode. Electroanal. 16(16): 1285–1291, http://dx.doi.org/10.1002/elan.200302955.

[13] Yuan, Y., Wang, J., Ni, X., Cao, Y. 2019. A biosensor based on hemoglobin immobilized with magnetic molecularly imprinted nanoparticles and modified on a magnetic electrode for direct electrochemical determination of 3-chloro-1,2-propandiol. J. Electroanal. Chem. 834(2018): 233–240, http://dx.doi.org/10.1016/j.jelechem.2018.12.034.

[14] Willyam, S.J., Saepudin, E., Ivandini, T.A. 2020. β-Cyclodextrin/Fe3O4 nanocomposites for an electrochemical non-enzymatic cholesterol sensor. Anal. Meth. 12(27): 3454–3461, http://dx.doi.org/10.1039/d0ay00933d.

[15] Xu Z., Fan X., Ma Q., Tang B., Lu Z., Zhang J., Mo G., Ye J., Ye J. 2019. A sensitive electrochemical sensor for simultaneous voltammetric sensing of cadmium and lead based on Fe3O4/multiwalled carbon nanotube/laser scribed graphene composites functionalized with chitosan modified electrode. Mater. Chem. Phys. 238(2018): 121877, http://dx.doi.org/10.1016/j.matchemphys.2019.121877.

[16] Nodehi, M., Baghayeri, M., Ansari, R., Veisi, H. 2020. Electrochemical quantification of 17α–Ethinylestradiol in biological samples using a Au/Fe3O4@TA/MWNT/GCE sensor. Mater. Chem. Phys. 244(January): 122687, http://dx.doi.org/10.1016/j.matchemphys.2020.122687.

[17] Li, D., Xu, Y., Zhang, L., Tong, H. 2014. A label-free electrochemical biosensor for acrylamide based on DNA immobilized on graphene oxide-modified glassy carbon electrode. Int. J. Electrochem. Sci. 9(12): 7217–7227.

[18] Yu, K., Kelly, K.L., Sakai, N., Tatsuma, T. 2008. Morphologies and surface plasmon resonance properties of monodisperse bumpy gold nanoparticles. Langmuir. 24(11): 5849–5854, http://dx.doi.org/10.1021/la703903b.

[19] Wilson, A.R., Sun, K., Chi, M., White, R.M., Lebeau, J.M., Lamb, H.H., Wiley, B.J. 2013. From core-shell to alloys: The preparation and characterization of solution-synthesized AuPd nanoparticle catalysts. J. Phys. Chem. C 117(34): 17557–17566, http://dx.doi.org/10.1021/jp404157m.

[20] Lee, S., Yoo, M., Koo, M., Kim, H.J., Kim, M., Park, S.K., Shin, D. 2013. In-house-validated liquid chromatography-tandem mass spectrometry (LC-MS/MS) method for survey of acrylamide in various processed foods from Korean market. Food Sci. Nutr. 1(5): 402–407, http://dx.doi.org/10.1002/fsn 3.56.

[21] Kim, M., Shin, S.W., Lim, C.W., Kim, J., Um, S.H., Kim, D. 2017. Polyaspartamide-based graft copolymers encapsulating iron oxide nanoparticles for imaging and fluorescence labelling of immune cells. Biomater. Sci. 5(2): 305–312, http://dx.doi.org/10.1039/c6bm00763e.

[22] Prabowo, M.H., Wibowo, A., Yuliani, F. 2012. Identifikasi dan analisis akrilamida dalam kopi serbuk (tubruk) dan kopi instan dengan metode kromatografi cair kinerja tinggi. J. Ilm. Farm. 9(1), http://dx.doi.org/10.20885/jif.vol9.iss1.art1.

[23] Rafael, C.E.D., Campanha, F.G., Vieira, L.G.E., Ferreira, L.P., David, P.O.T., Marraccini, P., Benassi, M.T.D. 2010. Evaluation of kahweol and

cafestol in coffee tissues and roasted coffee by a new high-performance liquid chromatography methodology. J. Agric. Food Chem. 58(1): 88–93, http://dx.doi.org/10.1021/jf9027427.

[24] Hufschmid, R., Arami, H., Ferguson, R.M., Gonzales, M., Teeman, E., Brush, L.N., Browning, N.D., Krishnan, K.M. 2015. Synthesis of phase-pure and monodisperse iron oxide nanoparticles by thermal decomposition. Nanoscale. 7(25): 11142–11154, http://dx.doi.org/10.1039/c5nr01651g.

[25] Xu, Z., Hou, Y., Sun, S. 2007. Magnetic core/shell Fe3O4/Au and Fe3O4/Au/Ag nanoparticles with tunable plasmonic properties. J. Am. Chem. Soc. 129(28): 8698–8699, http://dx.doi.org/10.1021/ja073057v.

[26] He, Y., Sheng, Q., Zheng, J., Wang, M., Liu, B. 2011. Magnetite-graphene for the direct electrochemistry of hemoglobin and its biosensing application. Electrochim. Acta. 56(5): 2471–2476, http://dx.doi.org/10.1016/j.electacta.2010.11.020.